Generating host-directed therapy options against COVID-19 using variational graph autoencoders

Sumanta Ray[1,†], Snehalika Lall[2,†], Anirban Mukhopadhyay[3,], Sanghamitra Bandyopadhyay[2,], Alexander Schönhuth[1,*]

[1] Genome Data Science, Faculty of Technology, Bielefeld University, Bielefeld, Germany
[2] Machine Inteligence Unit, Indian Statistical Institute, Kolkata, West Bengal 700108, India
[3] University of Kalyani, Kalyani, West Bengal, India.
[†]These authors contributed equally to the work.
[*]To whom correspondence should be addressed.
E-mail: as@cwi.nl

1 Node2vec: Sampling Strategy and Feature Matrix Generation

The principle of the feature learning framework of Node2Vec can be described as follows. Let $G = (V, E)$ be a graph, where V represents a set of nodes, and E represents the set of edges. The feature representation of nodes (V) is given by a mapping function: $f : V \rightarrow R^d$, where d specifies the feature dimension. Alternatively, f may be considered as a node feature matrix F of dimension of $|V| \times d$, where rows reflect the feature vectors $f(v)$. For each node, $v \in V$, a network neighborhood $NN_S(v) \subset V$ of node v is defined by employing a neighbourhood sampling strategy S. The sampling strategy can be sketched as an interpolation between breadth-first search and depth-first search [1], with objective function

$$\max_f \left(\sum_{v \in V} \log P(NN_S(v) \mid f(v)) \right) \tag{1}$$

This maximizes the likelihood of observing a network neighborhood $NN_S(v)$ for a node v given its feature representation $f(v)$. The probability of observing a neighborhood node $n_i \in NN_S(v)$ given $f(v)$ is

$$P(NN_S(v) \mid f(v)) = \prod_{n_i \in NN_S(v)} P(n_i \mid f(v)). \tag{2}$$

where n_i refers to the i^{th} neighbor of node v as part of $NN_S(v)$. Last, the conditional probability $P(n_i \mid f(v))$ of a neighborhood node $n_i \in NN_S(V)$ given the original node v is computed as the softmax the scalar product of their feature vectors $f(v)$ and $f(n_i)$

$$P(n_i \mid f(v)) = \frac{exp(f(v) \cdot f(n_i))}{\sum_{u \in V} exp(f(u) \cdot f(v))} \tag{3}$$

Neighborhood Sampling Strategy. Because exact computation of neighborhoods is too expensive, one needs to sample neighborhoods in an efficient way. Therefore, a flexible biased random walk procedure is employed. A random walk in a graph G is given by probabilities

$$P(a_i = x \mid a_{i-1} = v) = \pi(v, x), \tag{4}$$

Here, $\pi(v, x)$ is the transition probability between nodes v and x, where $(v, x) \in E$ and a_i is the i^{th} node in the walk of length l. The transition probability is given by $\pi(v, x) = c_{pq}(t, x) \times w_{vx}$, where t

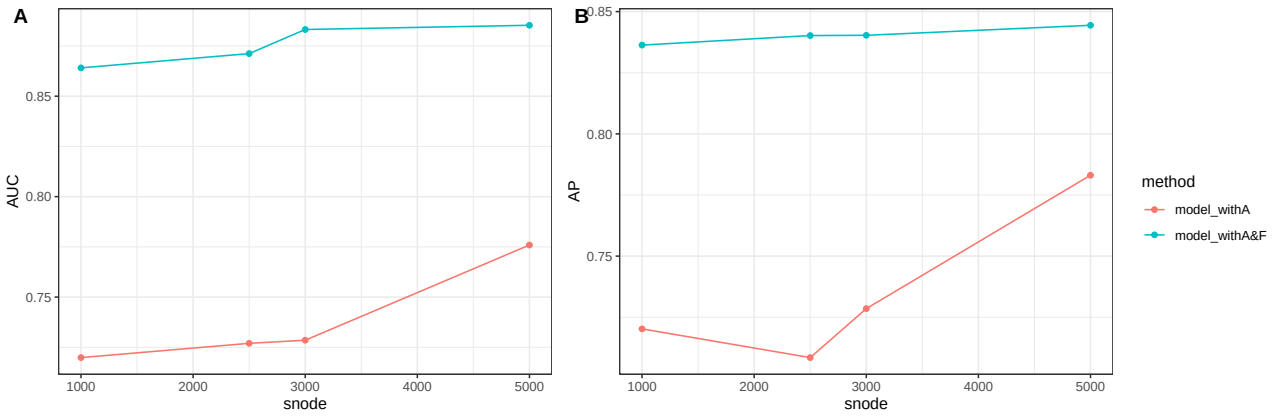

Figure 1. Performance of the model (AUC on the validation set) with and without using feature matrix (F)

2^*N_s	Average Performance on Validation Set		
	AUC (%)	AP (%)	Training Time (in sec)
7000	89.21 ± 0.02	85.32 ± 0.02	1587
5000	89.17 ± 0.03	85.30 ± 0.04	1259
3000	88.91 ± 0.10	85.02 ± 0.04	1026
2500	88.27 ± 0.15	84.88 ± 0.13	998
1000	86.69 ± 0.17	83.58 ± 0.19	816

Table 1. Average across the last 10 training epochs of FastGAE's validation AUC and AP for different numbers N_S of sampling nodes

is the previous node of v in the walk, w_{vx} is the (static) weight attached to the edge (v, x) and p, q are the two parameters that guide the walk. The coefficient $c_{pq}(t, x)$ is given by

$$c_{pq}(t,x) = \begin{cases} 1/p & \text{distance(t, x)=0} \\ 1 & \text{distance(t, x)=1} \\ 1/q & \text{distance(t, x)=2} \end{cases} \tag{5}$$

where distance(t, x) represents the distance of the shortest path between nodes t and node x.

As just pointed out, the process of feature matrix generation proceeds by applying the Node2vec algorithm. It starts from every node, simulating r random walks of fixed length l. In every step of a walk the transition probabilities $\pi(v, x)$ govern the sampling. In each iteration, generated walks are added to a list of walks. Each random walks forms a "sentence" that is ultimately used by word2vec [2], which takes a set of sentences (walks) as the neighborhood of the node, and outputs an embedding for each word, as described above. The log likelihood in equation 1 is optimized in the optimization step by employing a stochastic gradient descent algorithm on a two-layer Skip-gram neural network model used by word2vec.

2 Predicting Links using FastGAE: Details

Link Prediction. We utilize the scalable and fast version of variational graph autoencoders [3, FastVGAE] to reduce the computational time required by VGAE's in very large networks such as ours. The adjacency matrix A and the feature matrix F are fed into the encoder of FastVGAE as input. The encoder uses a graph convolution neural network (GCN) on the entire graph to create the

latent representation

$$Z = GCN(A, F) \tag{6}$$

The encoder works on the full adjacency matrix A. After encoding, one samples subgraphs, and decoding is performed on the sampled subgraphs.

The mechanism of the decoder of FastVGAE slightly differs from that of a traditional VGAE. For each subsample of graph nodes V_s, it regenerates an adjacency matrix $\widehat{A}$. For subsampling graph nodes, it makes use of a technique that determines the nodes from which to reconstruct the adjacency matrix in each iteration. Therefore, each node is assigned with a probability

$$p(i) = \frac{d(i)^\alpha}{\sum_{j \in V} d(j)^\alpha} \tag{7}$$

where $d(i)$ is the degree of node i, and α is the sharpening parameter, where in our study $\alpha = 2$. Nodes are then selected during subsampling according to their probabilities p_i until the subsampled nodes amount to $|V_s| = n_s$, the prescribed number of sampling nodes.

The decoder reconstructs the smaller matrix, $\widehat{A}_s$ of dimension $n_s \times n_s$ instead of decoding the main adjacency matrix A. The decoder function follows the following equation:

$$\widehat{A}_s(i, j) = \text{Sigmoid}(z_i^T \cdot z_j), \ \forall (i, j) \in V_s \times V_s \tag{8}$$

where z_i, z_j reflect the representations of nodes i, j, as computed by the encoder, see (6). At each training iteration a different subgraph (G_s) is drawn using the sampling method.

After training the model, the drug–CoV-host links are predicted using the equation

$$p(A_{ij} = 1 \mid z_i, z_j) = \text{Sigmoid}(z_i^T z_j), \tag{9}$$

where $A_{ij} = 1$ reflects a link between nodes i and j to exist, where i and j further reflect human proteins that interact with SARS-CoV-2 on the one hand and drugs on the other hand (recalling that we would like to predict links between human proteins that when targeted lead to the replication machinery of the virus falling apart). For each such combination of nodes the model computes the probability based on the logistic sigmoid function.

3 Repurposable Drugs and Targets: Categories, Details

Topoisomerase Inhibitors Topoisomerase Inhibitors such as Camptothecin, Daunorubicin, Doxorubicin, Irinotecan and Mitoxantrone are in the list of predicted drugs. The anticancer drug camptothecin (CPT) and its derivative Irinotecan have a potential role in antiviral activity [5]. Daunorubicin (DNR) is demonstrated as an inhibitor of HIV-1 virus replication in human host cells [6]. The anticancer antibiotic Doxorubicin was previously identified as a selective inhibitor of *in-vitro* Dengue and Yellow Fever virus [7]. Mitoxantrone shows antiviral activity against the human herpes simplex virus (HSV1) by reducing the transcription of viral genes in many human cells that are essential for DNA synthesis [8].

Histone Deacetylases Inhibitors (HDACi) Our predicted drug list (supplementary table-2) contains two HDACi: Scriptaid and Vorinostat. Both drugs can be used to achieve latency reversal in the HIV-1 virus safely and repeatedly [9]. Asymptomatic patients infected with SARS-CoV-2 are of significant concern as they are more vulnerable to infect large population than symptomatic patients. Moreover, in most cases (99-percentile), patients develop symptoms after an average of 5-14 days, which is longer than the incubation period of SARS and MERS. To this end, HDACi may serve as good candidates for recognizing and clearing the cells in which SARS-CoV-2 latency has been reversed.

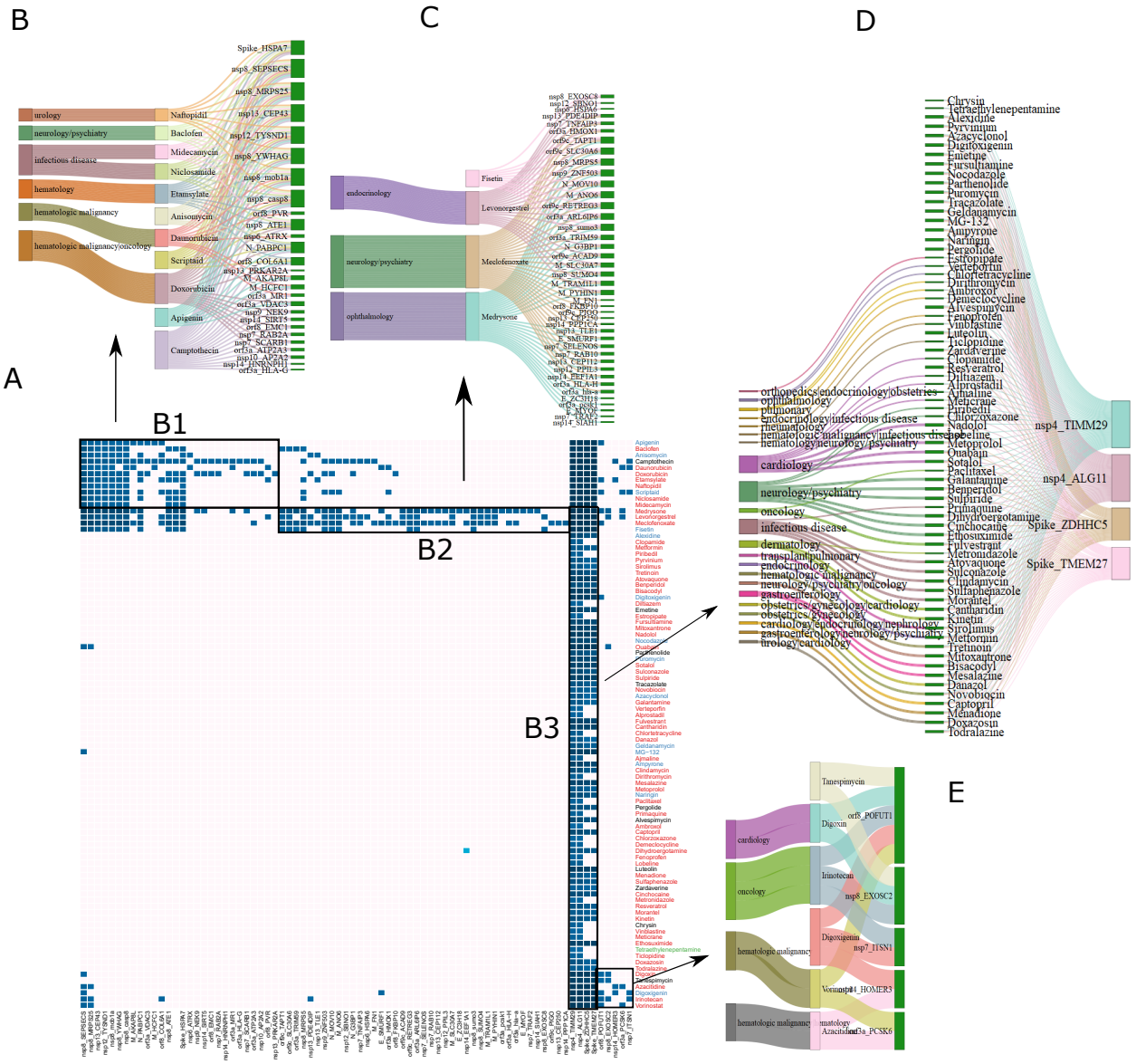

Figure 2. Drug–CoV-host predicted interaction: panel-A shows heatmap of probability scores between 92 drugs and 78 CoV-host proteins. The four predicted bipartite modules are annotated as B1, B2, B3 and B4 within the heatmap. The drugs are colored based on their clinical phase (red–launched, preclinical–blue, phase2/phase3–green and phase-1/ phase-2–black). Panel-B, C, D and E represents networks corresponding to B1, B2, B3 and B4 modules.The drugs are annotated using the disease area found in CMAP database [4]

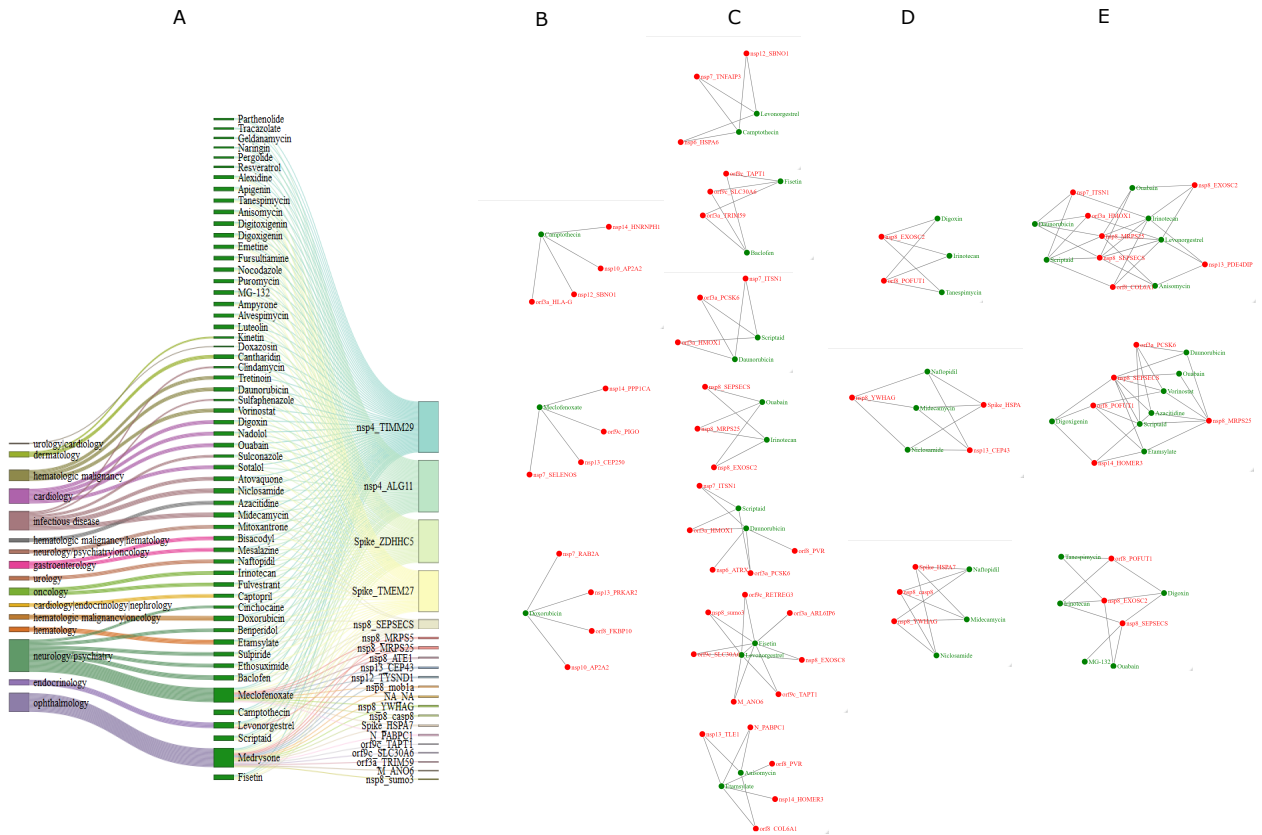

Figure 3. Predicted interactions for probability threshold: 0.9. panel-A shows the interaction graph between drugs and CoV-host. Drugs are annotated with their usage. Panel-B, C, D and E represents quasi-bicliques for one, two, three and more than three drugs molecules respectively.

HSP inhibitor Heat shock protein 90 (HSP) is described as a crucial host factor in the life cycle of several viruses that includes an entry in the cell, nuclear import, transcription, and replication [10, 11]. HSP90 is also shown to be an essential factor for SARS-CoV-2 envelop (E) protein [12]. In [13], HSP90 is described as a promising target for antiviral drugs. Predicted drug list contains three HSP inhibitors: Tanespimycin, Geldanamycin, and its derivative Alvespimycin. The first two have a substantial effect in inhibiting the replication of Herpes Simplex Virus and Human enterovirus 71 (EV71), respectively. Recently in [14], Geldanamycin and its derivatives are proposed to be an effective drug in the treatment of COVID-19.

Antimalarial agent, DNA-inhibitor, DNA methyltransferase/synthesis inhibitor Inhibiting DNA synthesis during viral replication is one of the critical steps in disrupting the viral infection. The list of predicted drugs contains six such small molecules/drugs, viz., Niclosamide, Azacitidine, Anisomycin, Novobiocin, Primaquine, Menadione, and Metronidazole (see supplementary text). Recently Hydroxychloroquine (HCQ), a derivative of CQ, has been evaluated to efficiently inhibit SARS-CoV-2 infection *in vitro* [15]. Therefore, another anti-malarial aminoquinolin drug Primaquine may also contribute to the attenuation of the inflammatory response of COVID-19 patients. Primaquine is already established to be effective in the treatment of Pneumocystis-pneumonia (PCP) [16].

Cardiac Glycosides ATPase Inhibitor The predicted list of drugs contains three cardiac glycosides ATPase inhibitors: Digoxin, Digitoxigenin, and Ouabain. These drugs have been reported to be effective against different viruses such as herpes simplex, influenza, chikungunya, coronavirus, and respiratory syncytial virus [17].

MG132, Resveratrol and Captopril MG132, a proteasomal inhibitor, is a strong inhibitor of SARS-CoV replication in early stage [18]. Resveratrol has also been demonstrated to be a significant inhibitor of MERS-CoV infections [19]. Another drug Captopril is known as Angiotensin II receptor blockers (ARB), which directly inhibits the production of angiotensin II. In [20], Angiotensin-converting enzyme 2 (ACE2) is demonstrated as the binding site for SARS-CoV-2. So Angiotensin II receptor blockers (ARB) may be good candidates to use in the tentative treatment for SARS-CoV-2 infections [21].

Table 2. 92 drugs predicted to be repurposable against SARS-CoV-2

Sl. No.	pubchem id	Drug	Clinical phase	Uses
1	15281	Alexidine	Preclinical	phosphatidylglycerophosphatase inhibitor
2	17150	Apigenin	Preclinical	casein kinase inhibitor—cell proliferation inhibitor
3	18998	Baclofen	Launched	benzodiazepine receptor agonist
4	33216	Clopamide	Launched	sodium/chloride cotransporter inhibitor
5	37446	Digoxin	Launched	ATPase inhibitor
6	107704	Digitoxigenin	Preclinical	ATPase inhibitor
7	117069	Ouabain	Launched	ATPase inhibitor
8	59105	Metformin	Launched	insulin sensitizer
9	71063	Piribedil	Launched	dopamine receptor agonist
10	220964	Pergolide	Withdrawn	dopamine receptor agonist
11	76299	Pyrvinium	Launched	androgen receptor antagonist
12	80626	Sirolimus	Launched	mTOR inhibitor
13	86324	Tanespimycin	Phase 3	HSP inhibitor
14	180858	Geldanamycin	Preclinical	HSP inhibitor
15	245370	Alvespimycin	Phase 2	HSP inhibitor

Table 2 continued from previous page

16	93086	Tretinoin	Launched	retinoid receptor agonist—retinoid receptor ligand
17	102361	Anisomycin	Preclinical	DNA synthesis inhibitor
18	103692	Atovaquone	Launched	mitochondrial electron transport inhibitor
19	104090	Azacitidine	Launched	DNA methyltransferase inhibitor
20	104487	Benperidol	Launched	dopamine receptor antagonist
21	121586	Sulpiride	Launched	dopamine receptor antagonist
22	104924	Bisacodyl	Launched	laxative
23	105316	Camptothecin	Phase 3	topoisomerase inhibitor
24	108903	Doxorubicin	Launched	topoisomerase inhibitor
25	114021	Irinotecan	Launched	topoisomerase inhibitor
26	115466	Mitoxantrone	Launched	topoisomerase inhibitor
27	107326	Daunorubicin	Launched	RNA synthesis inhibitor—topoisomerase inhibitor
28	108095	Digoxigenin	Preclinical	steroid
29	108477	Diltiazem	Launched	calcium channel blocker
30	109280	Emetine	Phase 2	protein synthesis inhibitor
31	118729	Puromycin	Preclinical	protein synthesis inhibitor
32	178082	Chlortetracycline	Launched	protein synthesis inhibitor
33	182249	Midecamycin	Launched	protein synthesis inhibitor
34	199663	Clindamycin	Launched	protein synthesis inhibitor
35	109651	Estropipate	Launched	estrogen receptor agonist
36	110088	Etamsylate	Launched	haemostatic agent
37	111183	Fursultiamine	Launched	vitamin B
38	114689	Medrysone	Launched	glucocorticoid receptor agonist
39	115901	Nadolol	Launched	adrenergic receptor antagonist
40	116238	Naftopidil	Launched	adrenergic receptor antagonist
41	119913	Sotalol	Launched	adrenergic receptor antagonist
42	215415	Metoprolol	Launched	adrenergic receptor antagonist
43	520283	Doxazosin	Launched	adrenergic receptor antagonist
44	116649	Nocodazole	Preclinical	tubulin polymerization inhibitor
45	220050	Paclitaxel	Launched	tubulin polymerization inhibitor
46	117480	Parthenolide	Phase 1	NFkB pathway inhibitor
47	119578	Scriptaid	Preclinical	HDAC inhibitor
48	124043	Vorinostat	Launched	HDAC inhibitor
49	120719	Sulconazole	Launched	sterol demethylase inhibitor
50	123302	Tracazolate	Phase 2	GABA receptor modulator
51	125857	Novobiocin	Launched	bacterial DNA gyrase inhibitor
52	129195	Azacyclonol	Preclinical	histamine receptor antagonist
53	133584	Galantamine	Launched	acetylcholinesterase inhibitor
54	139192	Niclosamide	Launched	DNA replication inhibitor—STAT inhibitor
55	145407	Verteporfin	Launched	photosensitizing agent
56	150553	Alprostadil	Launched	prostanoid receptor agonist
57	159244	Fulvestrant	Launched	estrogen receptor antagonist
58	176723	Cantharidin	Launched	protein phosphatase inhibitor
59	179449	Danazol	Launched	estrogen receptor antagonist—progesterone receptor agonist
60	186039	MG-132	Preclinical	proteasome inhibitor
61	191423	Ajmaline	Launched	sodium channel blocker

Table 2 continued from previous page

62	245766	Ambroxol	Launched	sodium channel blocker
63	352301	Cinchocaine	Launched	sodium channel blocker
64	193762	Ampyrone	Preclinical	cyclooxygenase inhibitor
65	203449	Dirithromycin	Launched	bacterial 50S ribosomal subunit inhibitor
66	212182	Levonorgestrel	Launched	estrogen receptor agonist—glucocorticoid receptor antagonist—progesterone receptor agonist—progesterone receptor antagonist
67	214498	Mesalazine	Launched	cyclooxygenase inhibitor—lipoxygenase inhibitor—prostanoid receptor antagonist
68	217727	Naringin	Preclinical	cytochrome P450 inhibitor
69	223747	Primaquine	Launched	antimalarial agent—DNA inhibitor
70	255979	Captopril	Launched	angiotensin converting enzyme inhibitor
71	260887	Chlorzoxazone	Launched	bacterial 30S ribosomal subunit inhibitor
72	268568	Demeclocycline	Launched	bacterial 30S ribosomal subunit inhibitor
73	270479	Dihydroergotamine	Launched	serotonin receptor agonist
74	279244	Fenoprofen	Launched	prostaglandin inhibitor
75	291604	Lobeline	Launched	acetylcholine receptor antagonist
76	293538	Luteolin	Phase 2	glucosidase inhibitor
77	295381	Meclofenoxate	Launched	nootropic agent
78	295680	Menadione	Launched	mitochondrial DNA polymerase inhibitor—phosphatase inhibitor
79	321706	Sulfaphenazole	Launched	dihydropteroate synthetase inhibitor
80	333068	Zardaverine	Phase 2	phosphodiesterase inhibitor
81	372869	Metronidazole	Launched	DNA inhibitor
82	416788	Resveratrol	Launched	cytochrome P450 inhibitor—SIRT activator
83	423536	Fisetin	Preclinical	Aurora kinase inhibitor
84	441851	Morantel	Launched	acetylcholine receptor agonist
85	451754	Kinetin	Launched	cell division inducer
86	461005	Chrysin	Phase 1	breast cancer resistance protein inhibitor
87	471412	Vinblastine	Launched	microtubule inhibitor—tubulin polymerization inhibitor
88	472841	Meticrane	Launched	diuretic
89	483385	Ethosuximide	Launched	succinimide antiepileptic
90	494980	Tetraethylenepentamine	Phase 2/Phase 3	superoxide dismutase inhibitor
91	517908	Ticlopidine	Launched	purinergic receptor antagonist
92	543633	Todralazine	Launched	antihypertensive agent

References

[1] A. Grover and J. Leskovec, "node2vec: Scalable feature learning for networks," in *Proceedings of the 22nd ACM SIGKDD international conference on Knowledge discovery and data mining*, 2016, pp. 855–864.

Table 3. Gene Ontology (biological process) and KEGG pathways for 78 CoV-host proteins

Term (GO/KEGG)	p-value	Genes
Herpes simplex infection	0.002142	TRAF2, PPP1CA, CASP8, HLA-A, HCFC1, HLA-G
Viral carcinogenesis	0.003507	TRAF2, YWHAG, CASP8, HLA-A, VDAC3, HLA-G
Endocytosis	0.006957	AP2A2, HLA-A, HSPA6, SMURF1, RAB10, HLA-G
Epstein-Barr virus infection	0.023579	TRAF2, HLA-A, TNFAIP3, HLA-G
Legionellosis	0.030506	EEF1A1, CASP8, HSPA6
Viral myocarditis	0.033704	CASP8, HLA-A, HLA-G
antigen processing and presentation (GO:0019882)	8.04E-05	HLA-H, HLA-A, MR1, RAB10, HLA-G
antigen processing and presentation of peptide antigen via MHC class I (GO:0002474)	2.60E-04	HLA-H, HLA-A, MR1, HLA-G
negative regulation of extrinsic apoptotic signaling pathway via death domain receptors (GO:1902042)	3.46E-04	TRAF2, HMOX1, CASP8, TNFAIP3
antigen processing and presentation of exogenous peptide antigen via MHC class I, TAP-independent (GO:0002480)	6.05E-04	HLA-H, HLA-A, HLA-G
negative regulation of I-kappaB kinase/NF-kappaB signaling (GO:0043124)	6.14E-04	TRIM59, CASP8, TLE1, TNFAIP3
cellular response to heat (GO:0034605)	0.010384	HMOX1, HSPA6, MYOF
nuclear polyadenylation-dependent tRNA catabolic process (GO:0071038)	0.020673	EXOSC8, EXOSC2
nuclear polyadenylation-dependent rRNA catabolic process (GO:0071035)	0.024756	EXOSC8, EXOSC2
antigen processing and presentation of exogenous peptide antigen via MHC class I, TAP-dependent (GO:0002479)	0.028411	HLA-H, HLA-A, HLA-G
type I interferon signaling pathway (GO:0060337)	0.02925	HLA-H, HLA-A, HLA-G
death-inducing signaling complex assembly (GO:0071550)	0.032873	TRAF2, CASP8
low-density lipoprotein particle clearance (GO:0034383)	0.032873	HMOX1, SCARB1
exonucleolytic trimming to generate mature 3'-end of 5.8S rRNA from tricistronic rRNA transcript (GO:0000467)	0.032873	EXOSC8, EXOSC2
U4 snRNA 3'-end processing (GO:0034475)	0.032873	EXOSC8, EXOSC2
interferon-gamma-mediated signaling pathway (GO:0060333)	0.035392	HLA-H, HLA-A, HLA-G
protein processing (GO:0016485)	0.036307	PCSK1, TYSND1, PCSK6
nuclear-transcribed mRNA catabolic process, exonucleolytic, 3'-5'(GO:0034427)	0.036907	EXOSC8, EXOSC2
regulation of sequestering of zinc ion (GO:0061088)	0.036907	SLC30A6, SLC30A7
regulation of immune response (GO:0050776)	0.038229	PVR, HLA-H, HLA-A, HLA-G

[2] T. Mikolov, I. Sutskever, K. Chen, G. S. Corrado, and J. Dean, "Distributed representations of words and phrases and their compositionality," in *Advances in neural information processing systems*, 2013, pp. 3111–3119.

[3] G. Salha, R. Hennequin, J.-B. Remy, M. Moussallam, and M. Vazirgiannis, "Fastgae: Scalable graph autoencoders with stochastic subgraph decoding," *Neural Networks*, 2021.

[4] A. Subramanian, R. Narayan, S. M. Corsello, D. D. Peck, T. E. Natoli, X. Lu, J. Gould, J. F. Davis, A. A. Tubelli, J. K. Asiedu *et al.*, "A next generation connectivity map: L1000 platform and the first 1,000,000 profiles," *Cell*, vol. 171, no. 6, pp. 1437–1452, 2017.

[5] S. B. Horwitz, C.-K. Chang, and A. P. Grollman, "Antiviral action of camptothecin," *Antimicrobial agents and chemotherapy*, vol. 2, no. 5, pp. 395–401, 1972.

[6] L. Filion, D. Logan, R. Gaudreault, and C. Izaguirre, "Inhibition of hiv-1 replication by daunorubicin." *Clinical and investigative medicine. Medecine clinique et experimentale*, vol. 16, no. 5, pp. 339–347, 1993.

[7] S. J. Kaptein, T. De Burghgraeve, M. Froeyen, B. Pastorino, M. M. Alen, J. A. Mondotte, P. Herdewijn, M. Jacobs, X. De Lamballerie, D. Schols *et al.*, "A derivate of the antibiotic doxorubicin is a selective inhibitor of dengue and yellow fever virus replication in vitro," *Antimicrobial agents and chemotherapy*, vol. 54, no. 12, pp. 5269–5280, 2010.

[8] Q. Huang, J. Hou, P. Yang, J. Yan, X. Yu, Y. Zhuo, S. He, and F. Xu, "Antiviral activity of mitoxantrone dihydrochloride against human herpes simplex virus mediated by suppression of the viral immediate early genes," *BMC microbiology*, vol. 19, no. 1, p. 274, 2019.

[9] N. M. Archin, J. L. Kirchherr, J. A. Sung, G. Clutton, K. Sholtis, Y. Xu, B. Allard, E. Stuelke, A. D. Kashuba, J. D. Kuruc *et al.*, "Interval dosing with the hdac inhibitor vorinostat effectively reverses hiv latency," *The Journal of clinical investigation*, vol. 127, no. 8, pp. 3126–3135, 2017.

[10] H.-Q. Ju, Y.-F. Xiang, B.-J. Xin, Y. Pei, J.-X. Lu, Q.-L. Wang, M. Xia, C.-W. Qian, Z. Ren, S.-Y. Wang *et al.*, "Synthesis and in vitro anti-hsv-1 activity of a novel hsp90 inhibitor bj-b11," *Bioorganic and medicinal chemistry letters*, vol. 21, no. 6, pp. 1675–1677, 2011.

[11] H. Y. Shim, X. Quan, Y.-S. Yi, and G. Jung, "Heat shock protein 90 facilitates formation of the hbv capsid via interacting with the hbv core protein dimers," *Virology*, vol. 410, no. 1, pp. 161–169, 2011.

[12] M. L. DeDiego, J. L. Nieto-Torres, J. M. Jiménez-Guardeño, J. A. Regla-Nava, E. Alvarez, J. C. Oliveros, J. Zhao, C. Fett, S. Perlman, and L. Enjuanes, "Severe acute respiratory syndrome coronavirus envelope protein regulates cell stress response and apoptosis," *PLoS pathogens*, vol. 7, no. 10, 2011.

[13] Y. Wang, F. Jin, R. Wang, F. Li, Y. Wu, K. Kitazato, and Y. Wang, "Hsp90: a promising broad-spectrum antiviral drug target," *Archives of virology*, vol. 162, no. 11, pp. 3269–3282, 2017.

[14] I. Sultan, S. Howard, and A. Tbakhi, "Drug repositioning suggests a role for the heat shock protein 90 inhibitor geldanamycin in treating covid-19 infection," *arXiv*, 2020.

[15] J. Liu, R. Cao, M. Xu, X. Wang, H. Zhang, H. Hu, Y. Li, Z. Hu, W. Zhong, and M. Wang, "Hydroxychloroquine, a less toxic derivative of chloroquine, is effective in inhibiting sars-cov-2 infection in vitro," *Cell discovery*, vol. 6, no. 1, pp. 1–4, 2020.

[16] H.-F. Vöhringer and K. Arastéh, "Pharmacokinetic optimisation in the treatment of pneumocystis carinii pneumonia," *Clinical pharmacokinetics*, vol. 24, no. 5, pp. 388–412, 1993.

[17] L. Amarelle and E. Lecuona, "The antiviral effects of na, k-atpase inhibition: A minireview," *International journal of molecular sciences*, vol. 19, no. 8, p. 2154, 2018.

[18] M. Schneider, K. Ackermann, M. Stuart, C. Wex, U. Protzer, H. M. Schätzl, and S. Gilch, "Severe acute respiratory syndrome coronavirus replication is severely impaired by mg132 due to proteasome-independent inhibition of m-calpain," *Journal of virology*, vol. 86, no. 18, pp. 10 112–10 122, 2012.

[19] S.-C. Lin, C.-T. Ho, W.-H. Chuo, S. Li, T. T. Wang, and C.-C. Lin, "Effective inhibition of mers-cov infection by resveratrol," *BMC infectious diseases*, vol. 17, no. 1, p. 144, 2017.

[20] J. Shang, G. Ye, K. Shi, Y. Wan, C. Luo, H. Aihara, Q. Geng, A. Auerbach, and F. Li, "Structural basis of receptor recognition by sars-cov-2," *Nature*, pp. 1–4, 2020.

[21] C. S. Biyani, V. Palit, and S. Daga, "The use of captopril—angiotensin converting enzyme (ace) inhibitor for cystinuria during covid-19 pandemic," *Urology*, vol. 141, pp. 182–183, 2020.